Available online at BCREC website: https://bcrec.id

Bulletin of Chemical Reaction Engineering & Catalysis, 15 (2) 2020, 525-537

**Research Article**

# CuAl LDH/Rice Husk Biochar Composite for Enhanced Adsorptive Removal of Cationic Dye from Aqueous Solution

**Neza Rahayu Palapa[1], Tarmizi Taher[2], Bakri Rio Rahayu[1], Risfidian Mohadi[3], Addy Rachmat[3], Aldes Lesbani[1,*]**

*[1]Graduate School of Mathematics and Natural Science Graduate School, Universitas Sriwijaya,*
*Jl. Padang Selasa, No. 524 Ilir Barat 1, Palembang, South Sumatra, Indonesia.*
*[2]Institute of Regional Innovation, Hirosaki University, Matsubara 2-1-3, 030-0813, Aomori City, Aomori, Japan.*
*[3]Department of Chemistry, Faculty of Mathematics and Natural Sciences, Universitas Sriwijaya,*
*Jl. Palembang-Prabumulih, Km. 32, Ogan Ilir, South Sumatra, Indonesia.*

*Received: 17th May 2020; Revised: 14th June 2020; Accepted: 14th June 2020;*
*Available online: 30th July 2020; Published regularly: August 2020*

## Abstract

The preparation of CuAl LDH and biochar (BC) composite derived from rice husk and its application as a low-cost adsorbent for enhanced adsorptive removal of malachite green has been studied. The composite was prepared by a one-step coprecipitation method and characterized by X-ray Diffraction (XRD), Fourier Transform Infra Red (FTIR), Brunauer-Emmett-Teller (BET), and Scanning Electron Microscopy - Energy Dispersive X-ray (SEM−EDX). The result indicated that CuAl LDH was successfully incorporated with the biochar that evidenced by the broadening of XRD peak at $2\theta = 24°$ and the appearance of a new peak at 1095 $\text{cm}^{-1}$ on the FTIR spectra. The BET surface area analysis revealed that CuAl/BC composite exhibited a larger surface area (200.9 $\text{m}^2/\text{g}$) that the original CuAl LDH (46.2 $\text{m}^2/\text{g}$). Surface morphological changes also confirmed by SEM image, which showed more aggregated particles. The result of the adsorption study indicated the composite material was efficient in removing malachite green with Langmuir maximum adsorption capacity of CuAl/BC reaching 470.96 mg/g, which is higher than the original CuAl LDH 59.523 mg/g. The thermodynamic analysis suggested that the adsorption of malachite green occurs spontaneously ($\Delta G < 0$ at all tested temperature) and endothermic nature. Moreover, the CuAl/BC composite showed strong potential as a low-cost adsorbent for cationic dye removal since it showed not only a high adsorption capacity but also good reusability.

***Keywords***: Adsorption; Biochar; Composite Material; Layered Double Hydroxide; Malachite Green

***How to Cite***: Palapa, N.R., Taher, T., Rahayu, B.R., Mohadi, R., Rachmat, A., Lesbani, A. (2020). CuAl LDH/Rice Husk Biochar Composite for Enhanced Adsorptive Removal of Cationic Dye from Aqueous Solution. *Bulletin of Chemical Reaction Engineering & Catalysis*, 15(2), 525-537 (doi:10.9767/bcrec.15.2.7828.525-537)

***Permalink/DOI***: https://doi.org/10.9767/bcrec.15.2.7828.525-537

## 1. Introduction

Layered double hydroxide (LDH) is a synthetic anionic clays mineral having the general formula $[M^{+2}_{1-x}M^{+3}_{x}(OH)_2]^{+}_{x}A_{x/n}^{-n}\cdot mH_2O$ [1]. $M^{2+}$ and $M^{3+}$ represent divalent and trivalent metal cation. The stacked of positive layers separated by interlamellar space consists of anions and water molecules [2−3]. Anions within the space act as counterbalancing and exchangeable species denote by $A^{-n}$, such as nitrate [4], carbonate,

---

* Corresponding Author.
E-mail: aldeslesbani@pps.unsri.ac.id (A. Lesbani)

sulfate [5], organic acid anions [6] and also inorganic anions [7−8]. LDH shows great potentials in various applications such as adsorption, membrane separation, catalysis, electrochemistry, and biomedicine [9–12].

The LDH advantages include high adsorption capacity, easy to prepare, extensive specific surface area, high flexibility, and excellent thermal stability [13]. The layers of LDH however, can be exfoliated during application hence cannot be reused [14]. Structure improvement therefore is needed particularly for adsorbent application by introducing supporting material, which improves the integrity of layers. Biochar i.e. an activated carbon made from biomass has been reported can be used in dyes removal [15]. Biochar is a pyrogenic black carbon that has been used as a carbon fixer in soil improvement and recently incorporated as supporting for increasing surface area of material [16]. BC has a high adsorption capacity, and a large surface area [17].

Advanced utilization of biochar on materials structure improvement was reported in LDH composite. The resulting composite used in removing contaminants within wastewater through the adsorption method [18−19]. Wan *et al.* [20] reported that phosphate successfully adsorbed by using Mg-Al and Mg-Fe bamboo BC. The adsorption achieved >95% phosphate removal within an hour [20]. Previously, Wang *et al.* [21] reported that arsenic adsorption using Ni-Fe pine BC composite has a maximum adsorption capacity 1.56 g/kg and 4.38 g/kg, respectively [21]. Meili *et al.* [19] reported the preparation of bone BC supported on Mg-Al LDH and used it on the removal of methylene blue. The maximum adsorption capacity attains 406 mg/g at 40 °C [19]. According to research, the presence of other supporting materials as composite LDH/BC gives the effect prevents agglomeration and improves the stability and some properties of the materials such as high performance adsorptive, sustainable and economical adsorbent materials [22]. Thus, LDH/BC has the potential to generate useful adsorbents with inherent and remarkable exchangeability of anion, high surface area, and less toxicity for organic contaminated wastewater treatment.

In the present work, we aimed to study the adsorption of malachite green using CuAl rice husk BC composite in aqueous solution. However, to the best of our knowledge, there is no report CuAl LDH composite to rice husk biochar as a removal agent of malachite green. The effect of various conditions including pH, time, initial concentration, temperature adsorption and reusability adsorbent effectivity were investigated in batch adsorption apparatus. Kinetic, isotherm, and thermodynamic adsorption of malachite green on composite material was discussed in this article.

## 2. Materials and Methods

### 2.1 Materials

The materials used in the experiment were copper nitrate trihydrate ($Cu(NO_3)_2.3H_2O$) (by Merck), aluminum nitrate nonahydrate ($Al(NO_3)_3.9H_2O$) (by Merck), sodium hydroxide (NaOH) (by Sigma Aldrich) and malachite green (by Merck). All those chemicals were pro-analysis grade. The rice husk biochar source was purchased from Bukata Organic Indonesia.

### 2.2 Preparation of CuAl/BC Composite

The CuAl/BC composite was prepared by developing our previously reported work [23]. CuAl/BC composite was prepared by coprecipitation method as follow: 10 mL of 0.75 M copper nitrate and 10 mL of 0.25 M aluminum nitrate (3:1) were mixed under vigorous stirring for an hour until the complete dissolution of the starting materials. The resulting mixtures were transferred to another beaker containing 1 g of the biochar under continuous stirring. As much as 4 M sodium hydroxide solution was added dropwise until the settlement formed at pH 10. The mixing solution was kept at 80 °C for three days. Composites were washed and dried at 40 °C for a day.

### 2.3 Material Characterization

X-ray diffraction pattern of the prepared adsorbent was recorded using XRD Rigaku Miniflex-600. The sample scanned at scan speed 1°/min from 2θ range 5–70°. Specific surface area was calculated by using Multipoint BET method based on data collected by ASAP Micromeritics 2020 at 77 K. Infrared spectra obtained from FTIR Shimadzu Prestige-21 that measured by KBr disc method and scanned at wavenumber range of 400−4000 $cm^{-1}$. The surface morphology of materials was characterized using SEM Quanta-650 Oxford instrument. The concentration of dye was analyzed using UV−Visible spectrophotometer Bio-Base BK-UV1800 at wavelength 619 nm.

### 2.4 Adsorption Study

The adsorption study was carried out using a batch system. The pH effect, the equilibrium time through the kinetics experiments, and the influence of temperature and concentration on the adsorption isotherm were investigated.

The effect of pH was investigated by adjusting pH 3 to 11 in the following procedure: 0.05 L of 25 mg/L malachite green solution with adjusted pH was placed in an Erlenmeyer. A 0.05 g of CuAl/BC composite was added into Erlenmeyer. The solution was shaken at 120 rpm by horizontal shaker at room temperature for two hours. After this time, the solution was centrifuged, and the concentration of malachite green determined by UV−Visible spectrophotometer at wavelength 619 nm.

The kinetic study was carried out by mixing 0.05 g of composite adsorbent with 0.05 L malachite green solution at pH 9 and room temperature in different initial concentrations. The kinetic parameters evaluated based on pseudo-first-order (PFO) and pseudo-second-order (PSO) approaches. The equation is written as follows Equations (1) and (2):

$$\log\left(q_e - q_t\right) = \log q_e - \left(\frac{k_1}{2.303}\right)t \tag{1}$$

$$\frac{t}{q_t} = \frac{1}{k_2 q_e^2} + \frac{1}{q_e}t \tag{2}$$

Note: $q_e$ is adsorption capacity at equilibrium (mg/g); $q_t$ is adsorption capacity at $t$ (mg/g); $t$ is adsorption time (min); $k_1$ is adsorption kinetic rate at pseudo-first-order (min$^{-1}$) and $k_2$ is adsorption kinetic rate at pseudo second-order (g/mg.min).

The isotherm and thermodynamic study were investigated by similar procedure as kinetic study. 0.05 g of composite adsorbent was mixed with 0.05 L malachite green solution at pH 9 in various temperatures and initial concentrations. The Langmuir isotherm models represented as the Equation (3) and Freundlich isotherm model written as Equation (4):

$$\frac{C}{m} = \frac{1}{q_m b} + \frac{C}{b} \tag{3}$$

$$\ln q_e = \ln k_F + \left(\frac{1}{n}\right)\ln C_e \tag{4}$$

where $C$ is a saturated concentration of adsorbate; $m$ is the amount of adsorbate; $q_m$ is the maximum adsorption capacity (mg/g), $b$ is the Langmuir constant (L/mg), $k_F$ is Freundlich constant and $n$ is Freundlich linear constant.

### 2.5 Reusability Study

The reusability test was aimed to investigate the durability of composite after long period of application. In this study, several reagents such as ethylenediaminetetraacetic acid, sodium chloride, water, sodium hydroxide, hydrochloride acid were used on the desorption process. Reusability evaluation carried out by mixing 0.05 g of composite adsorbent in 0.05 L malachite green 100 mg/L. The mixture was shaken for two hours, followed by filtration to separate the adsorbent from adsorbate. The adsorbent dried in oven while the adsorbate had its absorbance read. The dried adsorbent (CuAl/BC-MG LDH) reused by adding it in 0.025 L of HCl (0.01 M) follow by stirring for two hours and then dried in an oven. The dried material used in another adsorption test in a similar procedure, in which this procedure repeated three cycles of operations.

## 3. Results and Discussions

### 3.1 Adsorbent Characterization

The diffractogram of BC, CuAl LDH, and CuAl/BC composite was shown in Figure 1. The diffractogram CuAl/BC resembles the characteristic diffraction pattern of CuAl LDH and biochar. The intense peaks of CuAl LDH (JCPDS No. 37-0630) showed the peaks at 11.8°, 26.3°, 35.8°, 47.8°, 58.9°, and 63.1° corresponding to reflections of (003), (006), (012), (015), (110), and (116) which indicated the materials have layer structure [23]. Similar findings from CuAl LDH also exhibited in XRD pattern of CuAl/BC composite, although the intensity of LDH characteristic was decreased due to amorphous of biochar which would be enhancing the hydrophobic nature of the composite material [24]. The broad peak at 24° corresponding to

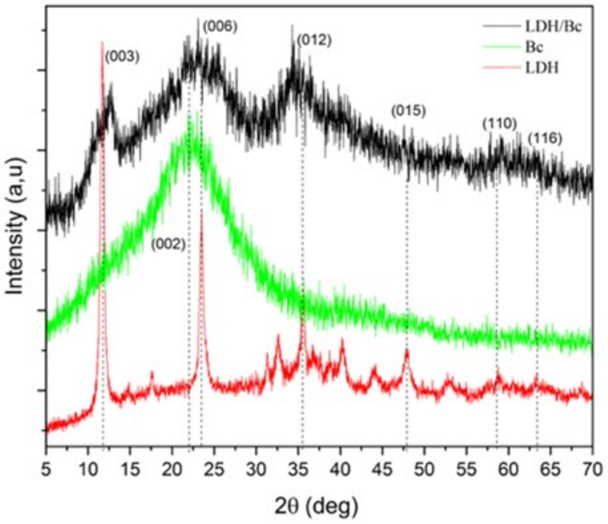

**Figure 1.** X-ray powder patterns of CuAl LDH, BC and CuAl/BC composite.

reflections (002) on the surface of the LDH due to the presence of biochar.

The FTIR spectra of biochar, LDH and composite presented in Figure 2. The characteristic band at 3448 cm$^{-1}$ and 1635 cm$^{-1}$ attributed to OH stretching vibrations and bending vibrations of the hydroxyl groups from water molecules. The band at 1000 cm$^{-1}$ belongs to the vibration of metal-oxygen. The bending vibration of nitrate appears at 1381 cm$^{-1}$ both on LDH pristine and composite. The absorption band at 1095 cm$^{-1}$ denotes the stretching vibration of C−O. The presence of these various absorption bands confirms the successful preparation of the composite LDH/BC.

The textural properties determination carried out by using $N_2$ adsorption-desorption method and the result presented in Table 1 while the adsorption isotherm shown in Figure 3. The value of BET surface area, pore size and pore volume listed in Table 1 shows that the increase of the surface area of LDH after supported by BC along with the decreases in pore size. The adsorption isotherms of each material shown in Figure 3. The isotherm curve showed type IV with a typical hysteresis loop, which is associated with capillary condensation within mesopore [25]. The hysteresis curve of these materials resemble to type H3. The H3 type hysteresis loop, according to IUPAC classification resulted from slit-shaped pores produced by aggregates of plate-like particles [26].

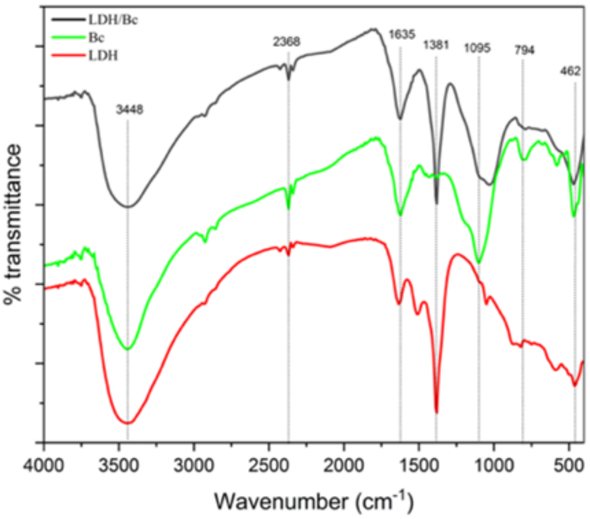

**Figure 2.** FTIR spectrum of CuAl LDH, BC and CuAl/BC composite.

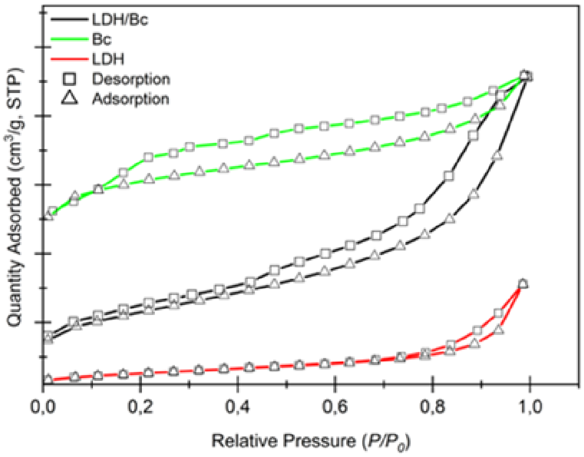

**Figure 3.** $N_2$ adsorption-desorption profile of CuAl LDH, BC and CuAl/BC composite.

The CuAl/BC composite resulted from this experiment shows a remarkable surface area according to BET calculation (200.9 m$^2$/g). Although the pore size of composite lower than initial LDH, its pore volume increases three times. The decrease in pore size probably due to the insertion of biochar particles within layers of LDH. Figure 4 suggests that biochar distributed on the surface of CuAl LDH, which confirms by Table 1, causes an increase in the surface area, and the occupation of the pores. The EDS supports the data as shown on Figure 4d. The pristine LDH of CuAl shows the composition of Cu and Al, *i.e.* 46% and 6%, respectively. Figure 4f. shows that composite consists of Cu, Al, C, O, Si at 35%, 5.1%, 11.2%, 39%, and 7.7%, respectively.

According to the previous report, the morphology of CuAl LDH pristine shows surface heterogeneity with large aggregate on its surface [23]. The LDH composite biochar exhibited a similar result reported by Wang *et al.* [27], which is the surface morphology of biochar modified LDH has no particular structure and predominantly reveals the presence of LDH phase.

Figure 5 shows the particle size distribution of CuAl/BC composite was obtained from ImageJ application 1.52q. The sample of CuAl/BC composite comprises of aggregates with the size of particles distributed from 9.09 μm to 54 μm. According to Sun *et al.* [28] the agglomeration of LDH particles causes the increase of

**Table 1.** BET surface area, BJH pore size and pore volume of the prepared materials.

| Materials | BET Surface (m$^2$/g) | Pore Size (nm) | Pore Volume (cm$^3$/g) |
|---|---|---|---|
| Biochar | 72.25 | 3.33 | 0.060 |
| CuAl | 46.2 | 10.39 | 0.116 |
| CuAl/BC composite | 200.90 | 7.03 | 0.350 |

particle size. The agglomeration can affect the particle size is a micro-scale magnitude [29]. On the other hand, the particle size of material results from varying pH and temperature during the synthesis process in the aqueous phase [30−31]. The average particle size of CuAl/BC composite is 28 µm.

### 3.2 Effect of pH

Figure 6 shows the effect of pH on the adsorption of malachite green by using CuAl LDH and CuAl/BC composite. The effective pH adsorption achieved at pH 9. The $pH_{pzc}$ of CuAl LDH is 8 and CuAl/BC composite is 6.8, at $pH_{pzc}$ the interaction between adsorbents and MG molecule is minimal due to absence of electrostatic forces. Thus, the high adsorption capacity at pH 9 possibly because the surface of these materials has a negative charge; hence the malachite green more likely to be absorbed. According to Parida & Mohapatra [32], at pH > pzc, the negative charge of surface material affects the interaction between positively molecule and surface become favored. An increase in pH makes malachite green removal occurred rapidly until pH at 9 and cationic dye occupied on the active site of the surface. At acidic conditions, the removal of malachite green using CuAl/BC composite and CuAl pristine achieved up to 40% removal if initial concentration was 25 mg/L. At higher pH the removal of malachite green increased up to >95 % and 99% for composite materials. This achievement can be attributed to the surface charge and the availability of binding sites exist on the surface of the composite, a characteristic predominantly belongs to the LDH [33]. Furthermore, the pH of adsorption process greatly affected the interaction of adsorbent and adsorbate, so, the next

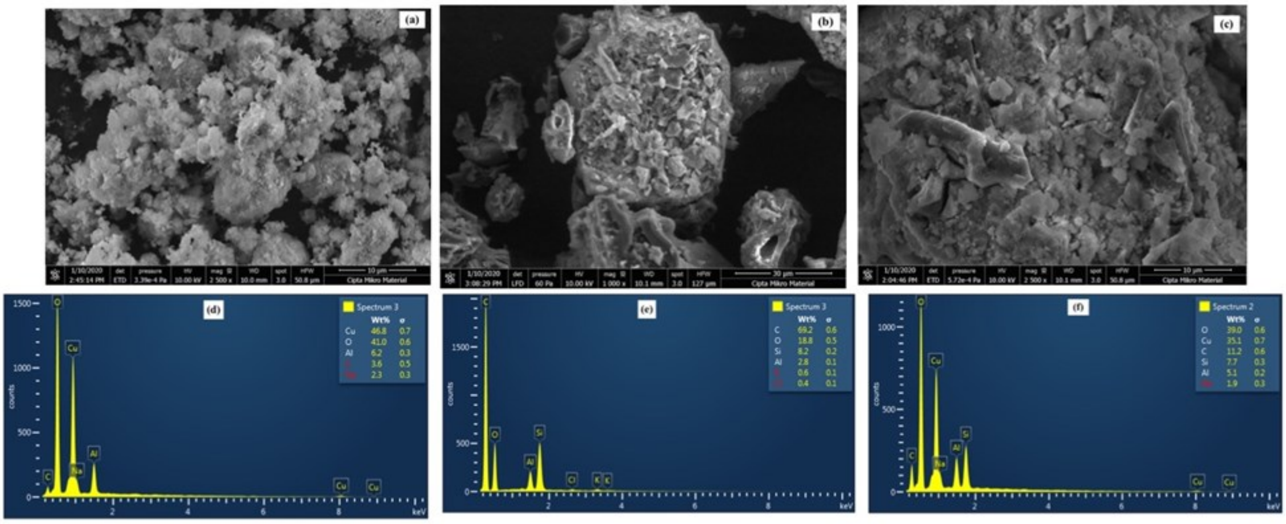

**Figure 4.** Morphologies and compositions of CuAl LDH (a,d), BC (b,e) and CuAl/BC composite (c,f).

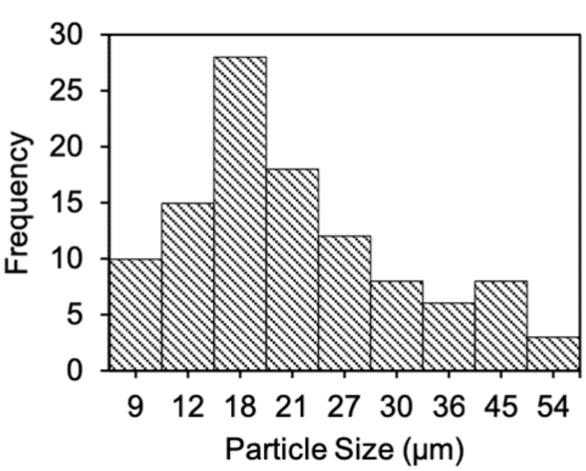

**Figure 5.** Distribution of particles size of CuAl/BC composite.

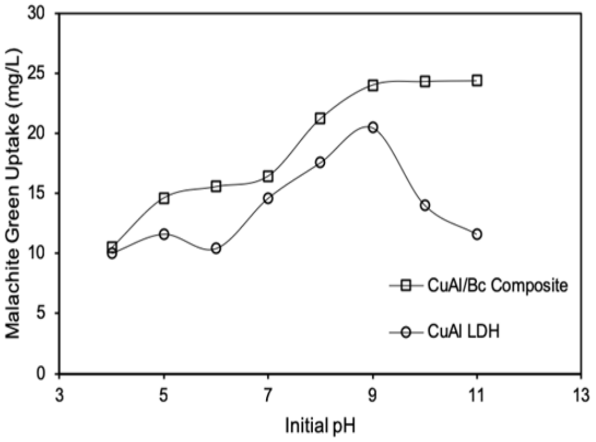

**Figure 6.** The effect of pH on adsorption of malachite green using CuAl/BC LDH and LDH pristine.

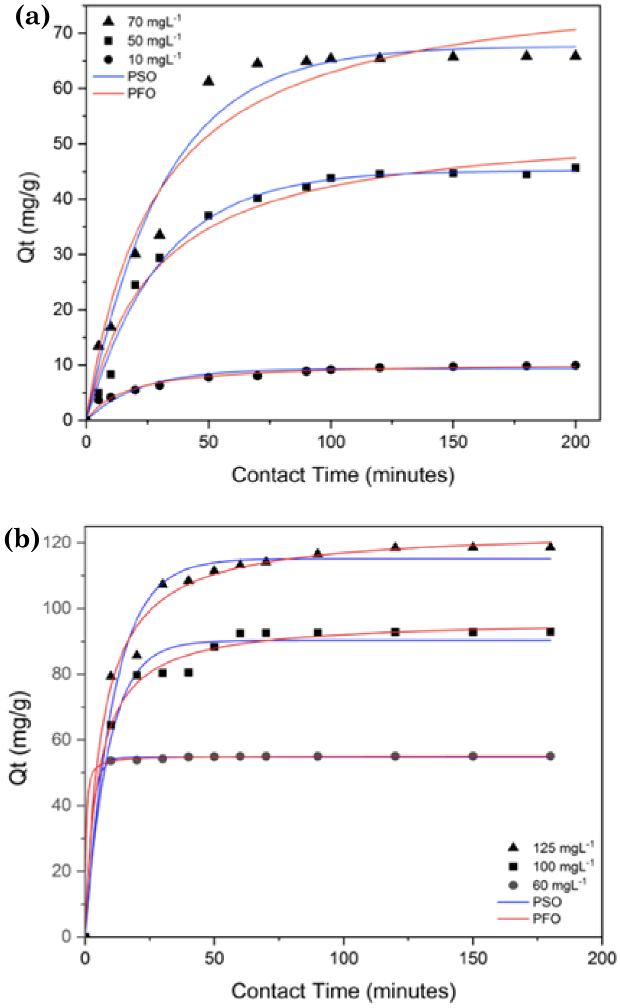

**Figure 7.** The effluent of contact time adsorption malachite green using (a) CuAl pristine and (b) CuAl/BC composite.

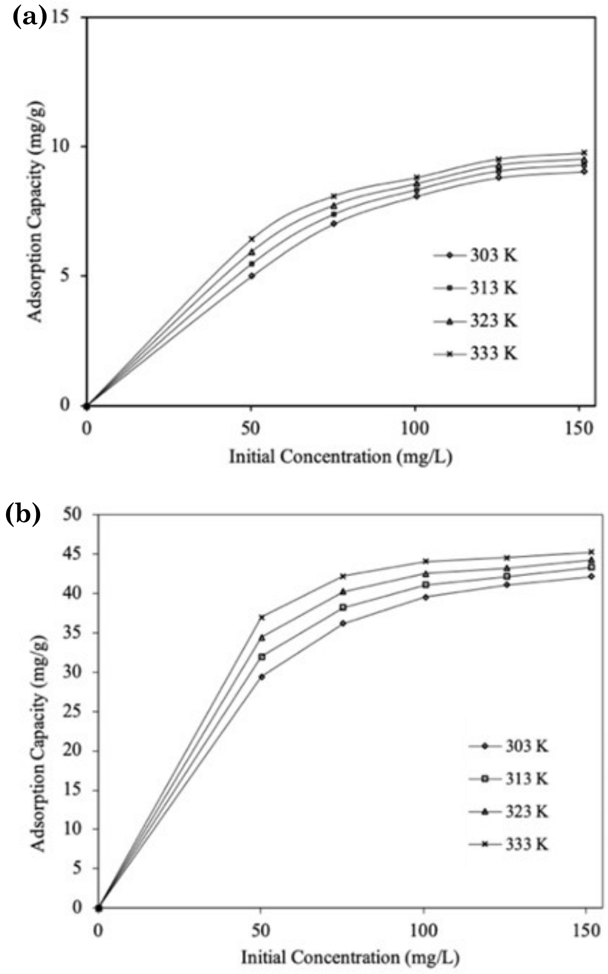

**Figure 8.** Effect of adsorption temperature in several initial concentration of Malachite green by using (a) CuAl pristine and (b) CuAl/BC composite.

**Table 2.** Kinetic parameters of CuAl LDH and CuAl/BC composite.

| Adsorbent | Initial Concentration (mg/L) | $Qe_{experiment}$ (mg/g) | PFO | | | PSO | | |
|---|---|---|---|---|---|---|---|---|
| | | | $Qe_{Calc}$ (mg/g) | $R^2$ | $k_1$ | $Qe_{Calc}$ (mg/g) | $R^2$ | $k_2$ |
| CuAl/BC composite | 60 | 34.476 | 31.69 | 0.975 | 0.038 | 34.246 | 0.999 | 0.119 |
| | 100 | 58.081 | 36.165 | 0.949 | 0.033 | 59.428 | 0.998 | 0.001 |
| | 125 | 74.125 | 53.801 | 0.967 | 0.048 | 76.124 | 0.998 | 0.001 |
| CuAl-LDH | 10 | 6.206 | 4.942 | 0.975 | 0.023 | 6.516 | 0.991 | 0.004 |
| | 50 | 16.446 | 20.265 | 0.987 | 0.043 | 27.350 | 0.968 | 0.001 |
| | 70 | 28.532 | 25.522 | 0.960 | 0.027 | 33.333 | 0.949 | 0.001 |

experiments of adsorption were conducted at pH 9.

### 3.3 Effect of Contact Time

The kinetic parameters were determined by varying contact time. Figure 7 shows the effect of contact time on the dye adsorption for both LDH and composite. The result showed that CuAl/BC composite adsorbed twice more dyes than CuAl LDH. This performance corresponded to the surface area of LDH composite, which is higher than pristine, as confirmed by BET analysis. Furthermore, Figure 7 informed that the adsorption equilibrium of malachite green reached after 90 minutes for LDH whereas the composite achieved at a shorter time *i.e.* 60 minutes. These results indicated that composite material showed a great potential adsorbent compare to pristine LDH. Pseudo first and second order (PFO and PSO) curves are shown in Figure 7 and the results of the kinetic parameter are presented in Table 2.

Table 2 shows the kinetic parameter of malachite green adsorption obtained from the calculation by using Equations 1 and 2 based on experimental data. Both materials were best represented by PSO kinetic model rather than the PFO that having the calculated equilibrium capacity close to equilibrium capacity from experimental ($Qe_{exp}$). The result acquired under the assumption that the difference between the concentration at the solid phase and equilibrium concentration might cause by the driving force. In this case, the adsorption by using composite observed experimentally faster than pristine LDH.

### 3.4 Effect of Temperature and Isotherm Adsorption

The adsorption isotherm of malachite green using CuAl LDH and CuAl/BC composite is shown in Figure 8. The increase in adsorption capacity can be related to the increase in temperature. The isotherm parameters were calculated by Langmuir and Freundlich isotherm model, as formulated by Equations (3) and (4). Table 3 presents the calculation results of the coefficient correlation, which identifies that the Langmuir model better fitted than the Freundlich model for composite material. A good fit of the Langmuir model indicates the adsorption process of the composite is monolayer with uniform energy distribution [34]. According to Meili *et al.* [19], the Langmuir process assumed that no significant interaction between adsorbate molecules. Thus, after dye particles occupied the active site, no further interaction occurs, particularly after the formation of monolayer [35].

Table 3 shows that the maximum adsorption capacity of CuAl/BC composite significantly increased up to 470.96 mg/g at 50 °C. The maximum adsorption capacity of CuAl/BC is larger than CuAl LDH. Thus, CuAl/BC composite displayed a high effectivity on malachite green adsorption. These findings confirm that composite material increases the dye adsorbed performance of LDH associated with the synergetic effect of biochar and CuAl LDH in the composite due to the surface area of CuAl/BC composite was bigger than pristine. The adsorption capacity increases with temperature. This tendency implies that adsorption occurs endothermically, particularly when involving

**Table 3.** Isotherm model of Malachite green adsorption using CuAl and CuAl/BC composite.

| LDH | Adsorption Isotherm | Adsorption Constant | *T* (K) | | | |
|---|---|---|---|---|---|---|
| | | | 303 | 313 | 323 | 333 |
| CuAl | Langmuir | $q_m$ | 42.31 | 51.04 | 53.68 | 59.523 |
| | | $B$ | 0.2191 | 0.314 | 0.44 | 0.2807 |
| | | $R^2$ | 0.9815 | 0.997 | 0.996 | 0.998 |
| | Freundlich | $n$ | 3.35 | 4.056 | 3.47 | 4.87 |
| | | $k_F$ | 7.812 | 19.611 | 17.67 | 28.86 |
| | | $R^2$ | 0.9099 | 0.98 | 0.99 | 0.984 |
| CuAl/BC | Langmuir | $q_m$ | 467.92 | 465.33 | 468.19 | 470.96 |
| | | $B$ | 0.085 | 0.0122 | 0.181 | 0.028 |
| | | $R^2$ | 0.997 | 0.997 | 0.998 | 0.998 |
| | Freundlich | $n$ | 4.93 | 5.92 | 7.71 | 10.36 |
| | | $k_F$ | 15.79 | 20.11 | 24.61 | 29.34 |
| | | $R^2$ | 0.946 | 0.950 | 0.944 | 0.937 |

LDH adsorbent, as reported by some authors [36−37]. The several adsorbents for malachite green adsorption were conducted by researchers are presented in Table 4. The adsorption capacity of the present work showed higher than reported by several authors. Hence, it can be concluded that the prepared CuAl/BC exhibited great potential as an adsorbent for malachite green.

### 3.5 Thermodynamic Study

The thermodynamic parameter is an important aspect on the adsorption process. The thermodynamic parameter evaluated according to the Van't Hoff equation. The equation is written as Equations (5) and (6):

$$\Delta G = -RT\ln\left(K_d\right) \tag{5}$$

$$\ln\left(K_d\right) = \frac{\Delta S}{R} - \frac{\Delta H}{RT} \tag{6}$$

$R$ is constant gases, and $K_d$ is the adsorption distribution coefficient. The parameters determined by plotting Van't Hoff linear regression with $1/T$ vs. ln ($K_d$). The linearity of adsorbents is shown in Figure 9.

Table 5 listed the value of the calculated thermodynamic parameters. The negative val-

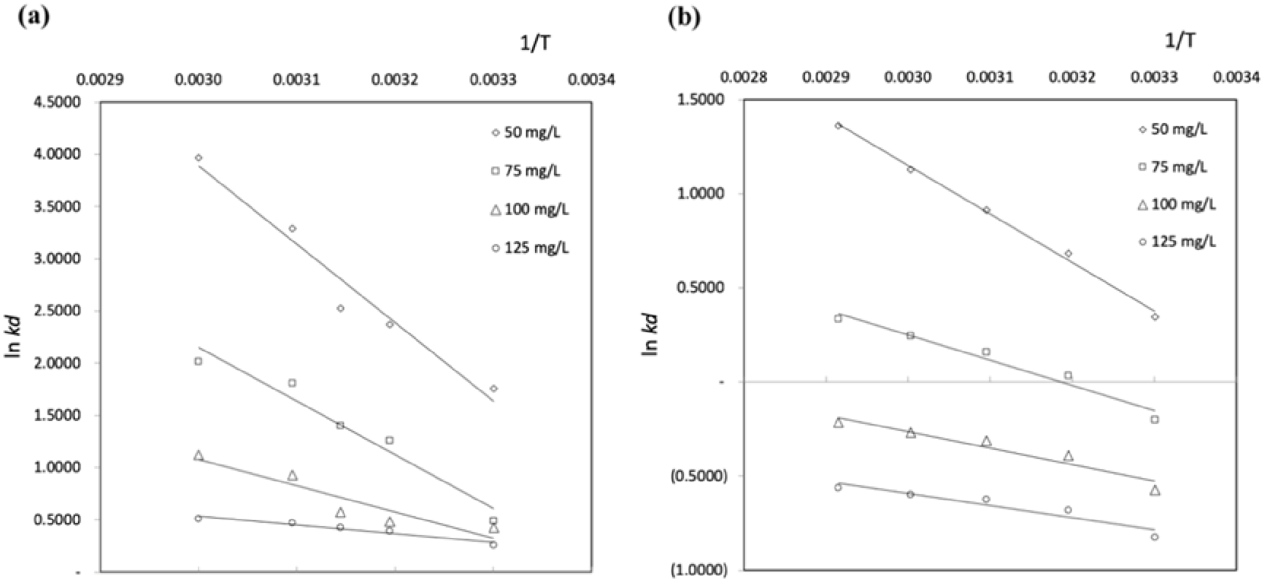

**Figure 9.** Van't Hoff linearity equation of malachite green adsorption using CuAl (a) and CuAl/BC composite (b).

**Table 4.** The comparison of adsorption capacity of malachite green by various adsorbents.

| Adsorbent | Adsorption Capacity (mg/g) | pH condition | Reference |
|---|---|---|---|
| Rice Husk BC | 32.6 | 9 | [15] |
| NiAl LDH | 73.38 | - | [41] |
| Sugarcane BC | 10 | - | [42] |
| CuCr LDH | 59.2 | 9 | [23] |
| Carbon coat LDH composite | 126.58 | 6 | [36] |
| Clayey soil | 78 | 6 | [43] |
| Lime peel activated carbon | 47 mg/g | - | [44] |
| *Manihot esculenta* BC | 932.98 | 6.98 | [45] |
| Magnetic BC *sewage* sludge | 388 | 7 | [46] |
| Fe-modified BC | 172.3 | 6 | [47] |
| Ternary Mg/Al+Fe LDH | 999.4 | 4 | [48] |
| CuAl/BC composite | 470.96 | 9 | Present Work |
| CuAl LDH | 59.523 | 9 | Present Work |

ue of ΔG at various temperatures denotes the spontaneity adsorption process and it is more favorable in high temperatures. The positive value of ΔS (30.702 kJ/mol and 20.071 kJ/mol) of MG adsorption using pristine CuAl LDH and composite corresponded to the randomness of solid-liquid phase interface during adsorption process [38]. Δ*H* the positive value indicated the reaction of adsorption become endothermic due to the MG adsorbed was increase with increasing temperature.

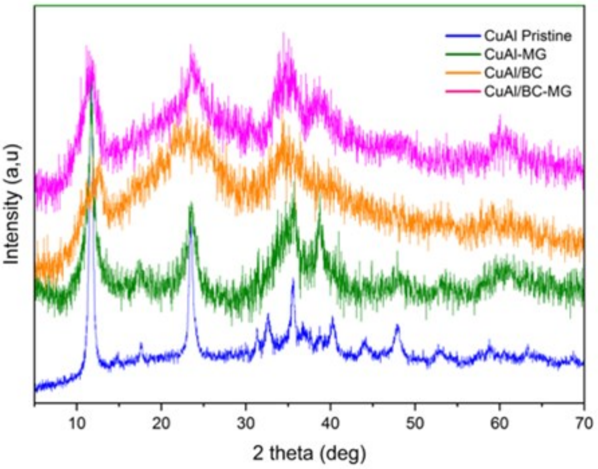

**Figure 10.** X-Ray diffraction powder of CuAl pristine, CuAl-MG, CuAl/BC composite, and CuAl/BC-MG.

### 3.6 Adsorption, Desorption, and Reusability Study

The solid structure of LDH and composite were evaluated by using X-Ray diffraction as shown in Figure 10. The diffractograms show similar pattern both LDH and composite before and after adsorption. The intensity in 2θ reflection (002) of CuAl/BC composite decreases after the adsorption process, and the interlayer of CuAl/BC composite slightly increases from 7.58 to 7.63 Å. This suggests the intercalation of malachite green within the LDH interlayer. According to Lu *et al.* [39], LDH interlayer after adsorption becomes smaller, but in this report, we obtain an increase in the interlayer distance as can be seen from peak shifting, which represents the (003). The enlargement of interlayer distance caused by malachite green intercalation within this layer [39].

In order to gain economic advantage as well as increase the effectiveness of potential adsorbent, the reusability study is necessary. The adsorbent reusability evaluation was carried out in several eluents on the desorption of malachite green from CuAl and CuAl/BC composite. The results are shown in Figure 11. The higher percent of desorption in acid solution perhaps corresponds to the LDH charge becomes positive, so, the electrostatic attraction of adsorbent-dye molecule and H-bond are weakened. Furthermore, in the base condition, the desorption is also higher because of hydro-

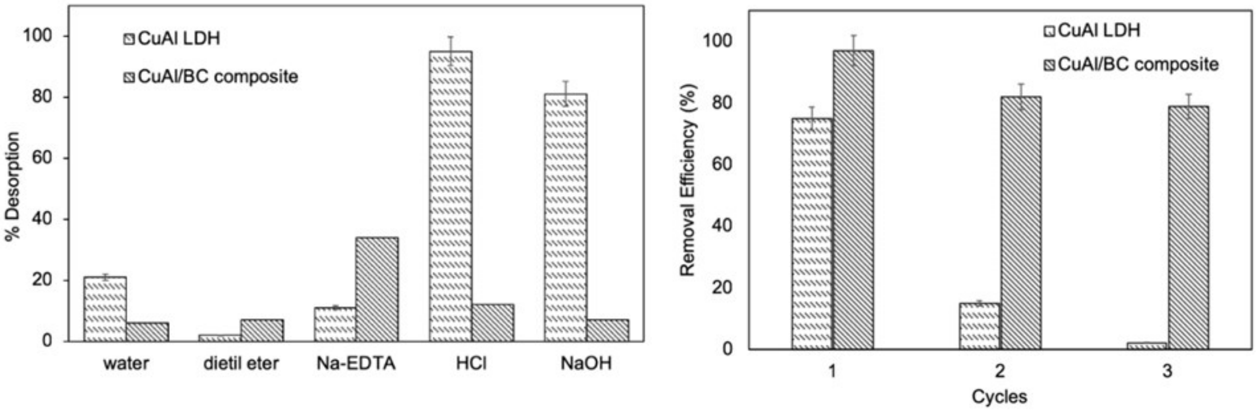

**Figure 11.** Desorption study by several eluent and reusability cycle of adsorbent.

**Table 5.** Thermodynamic parameters of CuAl and CuAl/BC composite.

| Adsorbent | Δ*G* (kJ/mol) | | | | Δ*S* (kJ/mol) | Δ*H* (kJ/mol) |
|---|---|---|---|---|---|---|
| | 303 K | 313 K | 323 K | 333 K | | |
| CuAl | -0.668 | -0.975 | -1.128 | -1.282 | 30.702 | 8.634 |
| CuAl/BC | -0.194 | -0.495 | -0.646 | -0.796 | 20.071 | 7.912 |

phobic interaction, and $OH^-$ ions are established to have a higher affinity for the anion exchange.

Figure 11 depicts that after three cycles of adsorption-desorption, the efficiency of dye removal decrease from 96 % to 78% for the composite and 72% to 2% for CuAl LDH. CuAl LDH dissolves in the acidic reagent hence not feasible to reuse. According to Nishimura *et al.* [40], LDH treated in regeneration processes might damage their structure due to exfoliation. However, the composite material prepared in this work can be reused, although the adsorption capacity slightly reduced.

## 4. Conclusions

The composite material of CuAl/BC has been successfully prepared and applied for cationic dye adsorption. The prepared materials were characterized by XRD, FTIR, BET and SEM-EDX. The XRD and FTIR peaks have confirmed the presence of characteristics of pristine materials. The morphology of CuAl/BC showed the heterogeneity with some aggregates from LDH. The surface area characterization of CuAl/BC evaluated the surface area increases four times from LDH pristine. Furthermore, CuAl/BC composite used as an adsorbent to remove the malachite green. The parameters of adsorption were determined using kinetic, isotherm, and thermodynamic parameters. The kinetic model of pseudo-second-order was appropriate for the composites with $q_e$ calculation and $q_e$ experiment is closed. The equilibrium adsorption MG using CuAl pristine was reached at 70 minutes with MG adsorbed 64.8 mg/L. The equilibrium of composite was reached at 40 minutes with MG adsorbed 108.92 mg/L. The isotherm adsorption follows Langmuir with maximum adsorption capacity 470.96 mg/g for composite compare to 59.523 mg/g for pristine. The thermodynamic analysis indicates that the malachite green adsorption in CuAl LDH and CuAl/BC composite were spontaneous ($\Delta G < 0$), endothermic (8.634 kJ/mol and 7.912 kJ/mol), the randomness of solid-liquid phase interface (30.702 kJ/mol and 20.071 kJ/mol) and that there was a little change in the adsorbent structure after adsorption. The regeneration study showed that three cycles adsorption process would reduce the adsorption capacity for LDH significantly but not for the composite material.

## Acknowledgment

Author would like to thanks to Universitas Sriwijaya, which provided funding through "*Hibah Profesi Dana PNPB*" in the fiscal year 2020 for supporting the financial of this research.

## References

[1] Bukhtiyarova, M.V. (2019). A review on effect of synthesis conditions on the formation of layered double hydroxides. *Journal of Solid State Chemistry*, 269, 494–506. DOI: 10.1016/j.jssc.2018.10.018

[2] Wang, Q., Hare, D.O. (2012). Recent Advances in the Synthesis and Application of Layered Double Hydroxide (LDH) Nanosheets. *Chemical Reviews,* 112, 7, 4124–4155. DOI: 10.1021/cr200434v

[3] Mishra, G., Dash, B., Pandey, S. (2018). Layered double hydroxides: A brief review from fundamentals to application as evolving biomaterials. *Appl. Clay Sci.*, 153, 172-186. DOI: 10.1016/j.clay.2017.12.021

[4] Antonyraj, C.A., Koilraj, P., Kannan, S. (2010). Synthesis of delaminated LDH: A facile two step approach. *Chemical Communications*, 46, 1902. DOI: 10.1039/b922122k

[5] Sepehr, M.N., Al-Musawi, T.J., Ghahramani, E., Kazemian, H., Zarrabi, M. (2017). Adsorption Performance of Magnesium/Aluminum Layered Double Hydroxide Nanoparticles for Metronidazole From Aqueous Solution. *Arabian Journal of Chemistry*, 10, 611–23. DOI: 10.1016/j.arabjc.2016.07.003

[6] Kameda, T., Takeuchi, H., Yoshioka, T. (2011). NiAl layered double hydroxides modified with citrate, malate, and tartrate: Preparation by coprecipitation and uptake of Cu 2 from aqueous solution. *Journal of Physics and Chemistry of Solids*, 72, 846–51. DOI: 10.1016/j.jpcs.2011.03.003

[7] Lesbani, A., Maretha, D.R., Taher, T., Miksusanti Mohadi, R., Andreas, R. (2018). Layered double hydroxides Mg/Fe intercalated H3[α-PW12O40]·n H2O as adsorbent of cadmium(II). *AIP Conference Proceedings*, 2049, 020013. DOI: 10.1063/1.5082418

[8] Sun, X., Dong, J., Li, Z., Liu, H., Jing, X., Chi, Y., Hu, C. (2019). Mono-transition-metal-substituted polyoxometalate intercalated layered double hydroxides for the catalytic decontamination of sulfur mustard simulant. *Dalton Transactions*, 48, 5285–5291. DOI: 10.1039/c9dt00395a

[9] Fu, F., Wang, Q. (2011). Removal of heavy metal ions from wastewaters: A review. *Journal of Environmental Management*, 92, 407–418. DOI: 10.1016/j.jenvman.2010.11.011

[10] Oktriyanti, M., Palapa, N.R., Mohadi, R., Lesbani, A. (2019). Modification Of Zn-Cr Layered Double Hydroxide With Keggin Ion. *Indonesian Journal of Environmental Management and Sustainability*, 3, 93–99.

[11] Zhu, J., He, J., Du, X., Lu, R., Huang, L., Ge, X. (2011). A facile and flexible process of ß-cyclodextrin grafted on Fe3O4 magnetic nanoparticles and host-guest inclusion studies. *Applied Surface Science*, 257, 9056–9062. DOI: 10.1016/j.apsusc.2011.05.099

[12] Qu, J., Sha, L., Wu, C., Zhang, Q. (2019). Applications of mechanochemically prepared layered double hydroxides as adsorbents and catalysts: A mini-review. *Nanomaterials*, 9, 1–15. DOI: 10.3390/nano9010080

[13] Zoromba, M.S., Nour, M.A., Eltamimy, H.E., Abd El-Maksoud, S.A. (2018). Effect of modified layered double hydroxide on the flammability and mechanical properties of polypropylene. *Science and Engineering of Composite Materials*, 25, 101–108. DOI: 10.1515/secm-2016-0050

[14] Ruan, X., Chen, Y., Chen, H., Qian, G., Frost, R.L. (2016). Sorption behavior of methyl orange from aqueous solution on organic matter and reduced graphene oxides modified Ni-Cr layered double hydroxides. *Chemical Engineering Journal*, 297, 295-303. DOI: 10.1016/j.cej.2016.01.041

[15] Leng, L., Yuan, X., Zeng, G., Shao, J., Chen, X., Wu, Z., Wang, H., Peng, X. (2015). Surface characterization of rice husk bio-char produced by liquefaction and application for cationic dye (Malachite green) adsorption. *Fuel*, 155, 77–85. DOI: 10.1016/j.fuel.2015.04.019

[16] Huang, D., Liu, C., Zhang, C., Deng, R., Wang, R., Xue, W., Luo, H., Zeng, G., Zhang, Q., Guo, X. (2019). Cr(VI) removal from aqueous solution using biochar modified with Mg/Al-layered double hydroxide intercalated with ethylenediaminetetraacetic acid. *Bioresource Technology*, 276, 127–132. DOI: 10.1016/j.biortech.2018.12.114

[17] Xu, X., Cao, X., Zhao, L. (2013). Comparison of rice husk- and dairy manure-derived biochars for simultaneously removing heavy metals from aqueous solutions: Role of mineral components in biochars. *Chemosphere*, 92, 955–961. DOI: 10.1016/j.chemosphere.2013.03.009

[18] Tareq, R., Akter, N., Azam, M.S. (2019). Biochars and Biochar Composites [Internet]. Biochar from Biomass Waste. Elsevier Inc. DOI: 10.1016/b978-0-12-811729-3.00010-8

[19] Meili, L., Lins, P.V., Zanta, C.L.P.S., Soletti, J.I., Ribeiro, L.M.O., Dornelas, C.B., Silva, T.L., Vieira, M.G.A. (2019). MgAl-LDH/Biochar composites for methylene blue removal by adsorption. *Applied Clay Science*, 168, 11–20. DOI: 10.1016/j.clay.2018.10.012

[20] Wan, S., Wang, S., Li, Y., Gao, B. (2017). Functionalizing biochar with Mg–Al and Mg–Fe layered double hydroxides for removal of phosphate from aqueous solutions. *Journal of Industrial and Engineering Chemistry,* 47, 246–253. DOI: 10.1016/j.jiec.2016.11.039

[21] Wang, S., Gao, B., Li, Y., Zimmerman, A.R., Cao, X. (2016). Sorption of arsenic onto Ni/Fe layered double hydroxide (LDH)-biochar composites. *RSC Advances*, 6, 17792–17799. DOI: 10.1039/c5ra17490b

[22] Li, H., Wen, J., Yu, R., Meng, J., Wang, C., Wang, C., Sun, S. (2015). Facile synthesis of a nanocomposite based on graphene and ZnAl layered double hydroxides as a portable shelf of a luminescent sensor for DNA. *RSC Advances*, 5, 9341–9247. DOI: 10.1039/C4RA15395B

[23] Palapa, N.R., Mohadi, R., Rachmat, A., Lesbani, A. (2020). Adsorption Study of Malachite Green Removal from Aqueous Solution Using Cu/M$^{3+}$(M$^{3+}$=Al,Cr ) Layered Double Hydroxide. *Mediterranean Journal of Chemistry*, 10, 33–45.

[24] Zubair, M., Jarrah, N., Khalid, A., Saood, M. (2018). Starch-NiFe-layered double hydroxide composites : Efficient removal of methyl orange from aqueous phase. *Journal of Molecular Liquids*, 249, 254–264. DOI: 10.1016/j.molliq.2017.11.022

[25] Szabados, M., Kónya, Z., Kukovecz, Á., Sipos, P., Pálinkó, I. (2019). Structural reconstruction of mechanochemically disordered CaFe-layered double hydroxide. *Applied Clay Science*, 174, 138–145. DOI: 10.1016/j.clay.2019.03.033

[26] Benito, P., Herrero, M., Labajos, F.M., Rives, V. (2010). Effect of post-synthesis microwave – hydrothermal treatment on the properties of layered double hydroxides and related materials. *Applied Clay Science*, 48, 218–227. DOI: 10.1016/j.clay.2009.11.051

[27] Wang, N., Sun, J., Fan, H., Ai, S. (2016). Anion-intercalated layered double hydroxides modified test strips for detection of heavy metal ions. *Talanta*, 148, 301–307. DOI: 10.1016/j.talanta.2015.11.007

[28] Sun, X., Neuperger, E., Dey, S.K. (2015). Insights into the synthesis of layered double hydroxide (LDH) nanoparticles: Part 1. Optimization and controlled synthesis of chloride-intercalated LDH. *Journal of Colloid and Interface Science*, 459, 264–272. DOI: 10.1016/j.jcis.2015.07.073

[29] Gunawan, P., Xu, R. (2009). Direct assembly of anisotropic layered double hydroxide (LDH) nanocrystals on spherical template for

fabrication of drug-LDH hollow nanospheres. *Chemistry of Materials*, 21(5), 781-783.

[30] Pang, X., Chen, L., Liu, Y., Chi, M., Li, Z., Plank, J. (2017). Growth behavior of water dispersed MgAl layered double hydroxide nanosheets. *RSC Advances*, 7, 14989–97. DOI: 10.1039/C7RA00833C

[31] Zhang, Q., Jiao, Q., Leroux, F., Tang, P., Li, D., Feng, Y. (2017). Antioxidant intercalated hydrocalumite as multifunction nanofiller for Poly(propylene): Synthesis, thermal stability, light stability, and anti-migration property. *Polymer Degradation and Stability*, 140, 9-16. DOI: 10.1016/j.polymdegradstab.2017.04.012

[32] Parida, K.M., Mohapatra, L. (2012). Carbonate intercalated Zn/Fe layered double hydroxide: A novel photocatalyst for the enhanced photo degradation of azo dyes. *Chemical Engineering Journal*, 179, 131–139. DOI: 10.1016/j.cej.2011.10.070

[33] Zhao, S., Xu, J., Wei, M., Song, Y.F. (2011). Synergistic catalysis by polyoxometalate-intercalated layered double hydroxides: Oximation of aromatic aldehydes with large enhancement of selectivity. *Green Chemistry*, 13, 384–389. DOI: 10.1039/c0gc00664e

[34] Darmograi, G., Prelot, B., Geneste, A., Martin-Gassin, A., Salles, F., Zajac, J. (2016). How does competition between anionic pollutants affect adsorption onto Mg-Al layered double hydroxide? Three competition schemes. *Journal of Physical Chemistry C*, 120, 10410–10418. DOI: 10.1021/acs.jpcc.6b01888

[35] Daud, M., Hai, A., Banat, F., Wazir, M.B., Habib, M., Bharath, G., Al-Harthi, M.A. (2019). A review on the recent advances, challenges and future aspect of layered double hydroxides (LDH)– Containing hybrids as promising adsorbents for dyes removal. *Journal of Molecular Liquids*, 288, 110989. DOI: 10.1016/j.molliq.2019.110989

[36] George, G., Saravanakumar, M.P. (2018). Facile synthesis of carbon-coated layered double hydroxide and its comparative characterisation with Zn-Al LDH: application on crystal violet and malachite green dye adsorption-isotherm, kinetics and Box-Behnken design. *Environmental Science and Pollution Research International*, 25, 30236–30254. DOI: 10.1007/s11356-018-3001-3

[37] Islam, M.A., Ali, I., Karim, S.M.A., Hossain Firoz, M.S., Chowdhury, A.N., Morton, D.W., Angove, M.J. (2019). Removal of dye from polluted water using novel nano manganese oxide-based materials. *Journal of Water Process Engineering*, 32, 100911. DOI: 10.1016/j.jwpe.2019.100911

[38] Yu, S., Wang, X., Chen, Z., Wang, J., Wang, S., Hayat, T., Wang, X. (2017). Layered double hydroxide intercalated with aromatic acid anions for the efficient capture of aniline from aqueous solution. *Journal of Hazardous Materials*, 321, 111–120. DOI: 10.1016/j.jhazmat.2016.09.009

[39] Lu, Y., Jiang, B., Fang, L., Ling, F., Gao, J., Wu, F., Zhang, X. (2016). High performance NiFe layered double hydroxide for methyl orange dye and Cr(VI) adsorption. *Chemosphere*, 152, 415–422. DOI: 10.1016/j.chemosphere.2016.03.015

[40] Nishimura, S., Takagaki, A., Ebitani, K. (2010). Monodisperse iron oxide nanoparticles embedded in Mg-Al hydrotalcite as a highly active, magnetically separable, and recyclable solid base catalyst. *Bulletin of the Chemical Society of Japan*, 83, 846–851. DOI: 10.1246/bcsj.20100059

[41] Lesbani, A., Tarmizi, R. D., Taher, T., Palapa, N. R., Mohadi, R. (2019). Preparation of Ni-Al LDH: Influence of intercalated polyoxometalate anion (α-$SiW_{12}O_{40}$) 4-on the interlayer gallery distance. *AIP Conference Proceedings*, 2194 (1), 020054. AIP Publishing

[42] Vyavahare, G.D., Gurav, R.G., Jadhav, P.P., Patil, R.R., Aware, C.B., Jadhav, J.P. (2018). Response surface methodology optimization for sorption of malachite green dye on sugarcane bagasse biochar and evaluating the residual dye for phyto and cytogenotoxicity. *Chemosphere*, 194, 306–315. DOI: 10.1016/j.chemosphere.2017.11.180

[43] Saha, P., Chowdhury, S., Gupta, S., Kumar, I. (2010). Insight into adsorption equilibrium, kinetics and thermodynamics of Malachite Green onto clayey soil of Indian origin. *Chemical Engineering Journal*, 165, 874–882. DOI: 10.1016/j.cej.2010.10.048

[44] Ahmad, M.A., Afandi, N.S., Bello, O.S. (2017). Optimization of process variables by response surface methodology for malachite green dye removal using lime peel activated carbon. *Applied Water Science*, 7, 717–727. DOI: 10.1007/s13201-015-0284-0

[45] Beakou, B.H., El Hassani, K., Houssaini, M.A., Belbahloul, M., Oukani, E., Anouar, A. (2017). A novel biochar from Manihot esculenta Crantz waste: Application for the removal of Malachite Green from wastewater and optimization of the adsorption process. *Water Science and Technology*, 76, 1447–56. DOI: 10.2166/wst.2017.332

[46] Zhang, J., Liu, M., Yang, T., Yang, K., Wang, H. (2016). A novel magnetic biochar from sewage sludge: Synthesis and its application for the removal of malachite green from wastewater. *Water Science and Technology*, 74, 1971–1979. DOI: 10.2166/wst.2016.386

[47] Kulaksiz, E., Gözmen, B., Kayan, B., Kalderis, D. (2017). Adsorption of Malachite Green on Fe-modified biochar: Influencing factors and process optimization. *Desalination and Water Treatment*, 74, 383–394. DOI: 10.5004/dwt.2017.20601

[48] Das, S., Dash, S.K., Parida, K.M. (2018). Kinetics, Isotherm, and Thermodynamic Study for Ultrafast Adsorption of Azo Dye by an Efficient Sorbent: Ternary Mg/(Al+Fe) Layered Double Hydroxides. *ACS Omega*, 3, 2532–2545. DOI: 10.1021/acsomega.7b01807